The American Journal of Pathology, Vol. 187, No. 4, April 2017

ELSEVIER

The American Journal of
PATHOLOGY
ajp.amjpathol.org

EPITHELIAL AND MESENCHYMAL CELL BIOLOGY

Cathepsin H—Mediated Degradation of HDAC4 for Matrix Metalloproteinase Expression in Hepatic Stellate Cells

Implications of Epigenetic Suppression of Matrix Metalloproteinases in Fibrosis through Stabilization of Class IIa Histone Deacetylases

Zemin Yang,* Yu Liu,* Lan Qin,† Pengfei Wu,* Zanxian Xia,‡ Mei Luo,*§ Yilan Zeng,§ Hidekazu Tsukamoto,† Zongyun Ju,¶ Danmei Su,* Han Kang,* Zhixiong Xiao,* Sujun Zheng,‖ Zhongping Duan,‖ Richard Hu,** Qiang Wang,†† Stephen J. Pandol,†† and Yuan-Ping Han*††

From The Center for Growth, Metabolism and Aging, and the Key Laboratory for Bio-Resource and Eco-Environment of Education of Ministry, College of Life Sciences, Sichuan University, Chengdu, China; the Department of Surgery,† University of Southern California, Los Angeles, California; the State Key Laboratory of Medical Genetics & School of Life Sciences,‡ Central South University, Changsha, China; the Chengdu Public Health Clinical Center,§ Chengdu, China; Chengdu Tongde Pharmaceutical Co. Ltd.,¶ Chengdu, China; Beijing YouAn Hospital,‖ Capital Medical University, Beijing, China; Olive View—UCLA Medical Center,** Los Angeles, California; and the Department of Medicine,†† Cedars-Sinai Medical Center, Los Angeles, California*

Accepted for publication December 8, 2016.

Address correspondence to Yuan-Ping Han, Ph.D., College of Life Sciences, Wanjiang Campus, Sichuan University, Chengdu, Sichuan Province, China, 6100065. E-mail: hanyp@scu.edu.cn.

In three-dimensional extracellular matrix, mesenchymal cells including hepatic stellate cells (HSCs) gain the ability to express matrix metalloproteinases (MMPs) on injury signals. In contrast, in myofibroblastic HSCs in fibrotic liver, many MMP genes are silenced into an epigenetically nonpermissive state. The mechanism by which the three-dimensional extracellular matrix confers the MMP genes into an epigenetically permissive state has not been well characterized. In continuation of previous work, we show here that the up-regulation of MMP genes is mediated through degradation of class IIa histone deacetylases (HDACs) by certain cysteine cathepsins (Cts). In three-dimensional extracellular matrix culture, CtsH, among other cysteine cathepsins, was up-regulated and localized as puncta in the nuclear and cytoplasmic compartments in a complex with HDAC4 for its degradation. Conversely, along with HSC *trans*-differentiation, CtsH and CtsL were progressively down-regulated, whereas HDAC4 was concurrently stabilized. The inhibition of cysteine cathepsins by specific proteinase inhibitors or chloroquine, which raises cellular pH, restored HDAC4. Recombinant CtsH could break down HDAC4 in the transfected cells and *in vitro* at acidic pH. In human cirrhotic liver, activated HSCs express high levels of class IIa HDACs but little CtsH. We propose that cysteine cathepsin—mediated degradation of class IIa HDACs plays a key role in the modulation of MMP expression/suppression and HSC functions in tissue injury and fibrosis. *(Am J Pathol 2017, 187: 781—797; http://dx.doi.org/10.1016/j.ajpath.2016.12.001)*

Supported by NIH grant DK069418 (Y.-P.H.); Department of Science and Technology, Sichuan Province, National Science Foundation of China grant 31571165 (Y.-P.H.); Chengdu Tongde Pharmaceutical Co. Ltd. (Y.-P.H.); National Key Research and Development Program of China grants 2016YFD0500300 and 2016YFC1200200 (Z.Xia); NIH grants P01CA163200-01 and P01DK098108 (S.J.P.); and NIH grants P50AA011999, R24AA012885, U01AA018663, and Department of Veteran Affairs grant I01BX001991 (H.T.).

Z.Y., Y.L., and L.Q. contributed equally to this work.

Disclosures: Z.J. and L.Q. are full-time employees of Chengdu Tongde Pharmaceutical Co. Ltd. (Sichuan, China) and Ambry Genetics (Aliso Viejo, CA), respectively. Tongde Pharmaceutical Co. Ltd. provided a small part of the funding for the final stage of the research.

Current address of L.Q., Ambry Genetics, Aliso Viejo, CA.

http://dx.doi.org/10.1016/j.ajpath.2016.12.001

Mesenchymal cells, such as fibroblasts in the dermis and stellate cells in the liver and pancreas, are spatially distributed in soft three-dimensional extracellular matrix (3D ECM) to gain and also maintain their architecture and functionality. In the liver, located in the space of Disse of the sinusoids, the hepatic stellate cells (HSCs) are ECM-producing cells of mesenchymal origin characterized by storage of vitamin A droplets.[1–3] Under certain physiologic or pathologic conditions, HSCs can adopt either a quiescent (q) HSCs or an activated phenotype, which is determined primarily by the nature of the surrounding microenvironment, including the mechanobiochemical interaction with the ECM and stimuli such as growth factors and cytokines. The qHSCs can express massive amounts of matrix metalloproteinases (MMPs) in response to injury signals for wound healing and repair.[4] For example, we have shown that in acute liver injury and driven by IL-1, the qHSCs can up-regulate MMP13 to release the cryptic and latent transforming growth factor β_1, which consequently terminates the ongoing inflammation through the induction of regulatory T cells.[5] Likewise, Toll-like receptor 4 signaling can also enhance transforming growth factor β signaling and hepatic fibrosis, showing a transition from injury to repair.[6] In persistent liver injury, such as chronic hepatic viral infection or long-term alcohol or xenobiotic exposure, and driven by growth factors such as transforming growth factor β and fibrotic-type ECM, the qHSCs can undergo *trans*-differentiation to acquire myofibroblast-like phenotypes.[7] In a dramatic manner, the injury type of MMP genes (including 10 MMP genes clustered in the far arm of chromosome 8, and *MMP9* in chromosome 3) are suppressed/silenced in the myofibroblastic HSCs to favor ECM accumulation and fibrosis.[4] Remarkably, in the myofibroblastic HSCs, the key signal-transduction pathways involved in the activation of MMP gene transcription, such as the c-Jun N-terminal kinase and Iκ kinase pathways, are not down-regulated or impaired.[8] These results suggest that the suppression of the MMP genes in the myofibroblastic HSCs may be mediated by an epigenetic mechanism rather than by failed signal transduction. Indeed, by chromatin immune precipitation, we showed that the promoter regions of the MMP genes are inaccessible to transcription factors, due to impairment of histone acetylation and failed recruitment of RNA polymerase II.[8] In this regard, we predicted that the great capacity of qHSCs to express MMPs in 3D ECM is regulated through a permissive epigenetic mechanism, in contrast to the nonpermissive epigenetic state in tissue fibrosis, by which the MMP genes are suppressed.

Histone deacetylases (HDACs), through hydrolysis of acetyl residues from ε-amine groups of proteins such as histones, are involved in the epigenetic suppression of gene expression in diverse cellular functions.[9] Based on sequence similarities and structural features, HDACs are classified into four families (classes I, IIa, IIb, and IV).[10] The potential role of HDACs in tissue fibrosis is emerging.[11] Specifically, HDAC4 is a class IIa HDAC a mostly potent for driving the transforming growth factor β–mediated formation of myofibroblasts.[12] A class II–specific HDAC inhibitor is able to suppress myofibroblast activation, in part through up-regulation miR-29.[13] We have previously shown that in the course of HSC *trans*-differentiation, the protein levels of class IIa HDACs are progressively increased and stabilized.[8] Moreover, we found that overexpression of HDAC4 efficiently suppressed *MMP9/13* expression in the HSCs. In the present study, we addressed how the class II HDACs are down-regulated by the mesenchymal cells, including HSCs grown in the 3D ECM tissue environment, which consequently confers multiple MMP genes into an epigenetic permissive state for their expression on injury signals. Conversely, we also proposed a mechanism by which class II HDACs are accumulated in the myofibroblastic HSCs or mesenchymal cells grown on rigid interface, leading to MMP suppression in tissue fibrosis.

Materials and Methods

Reagents

Recombinant human tumor necrosis factor (TNF)-α (210-TA), recombinant human cathepsin (Cts)-H protein (7516-CY-010), and CtsL protein (952-CY) were purchased from R&D Systems (Minneapolis, MN). Type I collagen (5005) was purchased from Advanced BioMatrix (San Diego, CA). Collagenase (195109) was purchased from MP Biomedicals (Santa Ana, CA). MG132, E64, antibody kit for HDACs (9928), histone H3 (9715), and histone H4 (2592) were purchased from Cell Signaling Technology (Beverly, MA). Antibodies against CtsH (N-18; sc-6496), CtsL (C-18), and other cathepsins; green fluorescent protein (B-2); p21 (C-19); and horseradish peroxidase–conjugated secondary antibodies (sc-2020, sc-2005, and sc-2004) were purchased from Santa Cruz Biotechnology (Dallas, TX). The antibodies for α–smooth muscle actin (F3777) and FLAG tag (M2) (Sigma-Aldrich, St. Louis, MO) were gifts from Prof. Li Qintong (Sichuan University, Sichuan, China). Antibodies against glyceraldehyde-3-phosphate dehydrogenase (7E4), β-actin (6D7), and hemagglutinin tag (3C6) were purchased from Zen BioScience (Chengdu, China).

Human Cirrhotic Liver Tissue

The protocol for collecting human liver tissue samples was approved by the IRB at Keck School of Medicine, University of Southern California (Los Angeles, CA) (Y.-P.H.). The specimens with advanced cirrhosis, as determined by a pathologist, were mostly derived from hepatitis C virus–infected patients ($n = 10$), and tissues were frozen in liquid nitrogen and embedded in OCT compound for immunofluorescence microscopy analysis.

Isolation of Rat HSCs

HSCs were isolated from male Wistar rats (Charles River Laboratories International, Wilmington, MA) by Integrative Liver Cell Core, Southern California Research Center for ALPD and Cirrhosis (protocol number 5R24AA012885), University of Southern California. The animal protocol was approved by the Institutional Animal Care and Use Committee at Keck School of Medicine, University of Southern California (Y.-P.H.). The normal Wistar rats were treated by *in situ* sequential digestion with Pronase (Roche Applied Science, Indianapolis, IN) and collagenase, followed by arabinogalactan gradient ultracentrifugation as described previously.[4] Briefly, the liver was sequentially digested with Pronase and type IV collagenase (Sigma-Aldrich) by *in situ* perfusion. Parenchymal cells were removed by centrifugation of the digestion at 50 × *g* for 2 minutes, and the subsequent nonparenchymal cells were laid on top of the four density gradients of arabinogalactan (Sigma-Aldrich). The gradients were generated through centrifugation at 100,000 × *g* for 40 minutes at 25°C using a SW41 Ti Rotor (Beckman Instruments, Brea, CA). A pure fraction of HSCs was recovered from the interface between the medium and the density of 1.035. The purity of HSCs was assessed by phase contrast microscopy and UV-excited fluorescence microscopy for vitamin A droplets, and the viability was examined by the trypan blue exclusion test.

3D ECM Cell Culture Model

Freshly isolated rat HSCs, and cells from lines including NIH/3T3, Cos7, and HEK-293 and HEK-293T, were seeded on 24-well cell culture plates (5×10^5 cells/well) with Dulbecco's modified Eagle's medium (DMEM) (10% fetal bovine serum) as a control. Type I collagen gel cocktail was mixed as described previously.[4] Briefly, this cocktail was prepared by mixing 0.3 mL of 10× MEM, 0.3 mL of 0.1 NaOH, 0.7 mL of DMEM, 1.0 mL of cell suspension in DMEM, and 2.4 mL of type I collagen (2.9 mg/mL). Then, 0.5 mL of gel cocktail was added in the 24-well plates (5×10^5 cells/well) as 3D ECM culture. After polymerization at 37°C for 60 minutes, the DMEM containing 10% fetal bovine serum was gently added on top of the gel, and the plates were incubated at 37°C with 5% CO_2.

Plasmids, Transfection, Viral Infections, and RNA Interference

Expression plasmids including FLAG-tagged pcDNA3-HDAC4, pcDNA3-HDAC4 ΔCter (1-359), pcDNA3-HDAC4 ΔNter (359-1076), pcDNA3-HDAC4 (L1062A),[14] pExpress-CTSH, pExpress-CTSH (C139S), and pExpress-HA-CTSH were prepared according to standard protocols.[15] The point mutation variants of HDAC4 (L1062A) and CtsH (C139S) were generated by PCR-based site-directed mutagenesis methods. Briefly, plasmid DNA with an insert of interest was used as a template. The oligonucleotide primers containing the desired mutations and each complementary to opposite strands of the vector were extended during temperature cycling by *Thermococcus kodakaraensis* DNA polymerase. After the temperature cycling, PCR product was treated by *Diplococcus pneumoniae*–derived I endonuclease, and parental methylated DNA was digested. The remaining nicked DNA containing the desired mutations was transformed into and amplified in *Escherichia coli* cells. The mutations of the constructs were confirmed through DNA sequencing analysis. The primers for cloning are listed in Table 1. *Lentivirus* spp were amplified by cotransfection of HEK-293T cells with psPAX2, pMD2-G packaging plasmid, and the lentiviral expression plasmids (pLVX puro-HDAC4, pLVX puro-CtsH, pLKO.1 shCtsH, and pLKO.1 shGFP). Murine CtsH shRNAs were cloned into pLKO.1 (Clontech Laboratories, Mountain View, CA), and the target sequences were shCtsH1, 5′-AAGGAA-GATTCAAGCCCACAA-3′; and shCtsH2, 5′-AAGGAAC-CACACATTTAAAAT-3′.[16] The shRNA against Green fluorescent protein being derived from Thermo Fisher Scientific (Waltham, MA) was used as a control. Cos7, NIH/3T3, HEK-293, and HEK-293T cells were transfected by particular plasmids through Lipofectamine 2000 (InvitroGen, Carlsbad, CA) according to the manufacturer's instructions.

Real-Time Quantitative RT-PCR Analysis

Total RNA of cell culture was extracted using TransZol reagent (Beijing TransGen Biotech Co, Ltd, Beijing, China) according to the manufacturer's instructions. Reverse transcription was performed with an RT kit (Takara Bio, Tokyo, Japan) according to the manufacturer's instructions. Real-time quantitative PCR was performed using SYBR Green Master Mix (Bio-Rad Laboratories, Segrate, Italy). Each

Table 1 Primers Used for Cloning

Primer	Forward primer	Reverse primer
pcDNA3-FLAG-*HDAC4* ΔCter (1-359)	5′-GGAATTCGCCACCATGGACTACAAGGACGAC-GACGACAAGAGCTCCCAAAGCCATCCA-3′	5′-AAGGAAAAAAGCGGCCGCTTAGGCAGGA-AGTCCCAAGGT-3′
pcDNA3-FLAG-*HDAC4* ΔNter (359-1076)	5′-GGAATTCGCCACCATGGACTACAAGGACGAC-GACGACAAGACTGGCCCTGCCGCTGGT-3′	5′-AAGGAAAAAAGCGGCCGCCAGTGTGAT-3′
pcDNA3-*HDAC4* (L1062A)	5′-CCGCCATGGCCTCGGCGTCTGTAGGCGTCA-3′	5′-TGACGCCTACAGACGCCGAGGCCATGGCGG-3′
pExpress-*CTSH* (C139S)	5′-GGGGCCTGTGGCAGCAGCTGGACTTTCTCTA-3′	5′-TAGAGAAAGTCCAGCTGCTGCCACAGGCCCC-3′

Table 2 Primers Used for RT-qPCR Analysis

Name	Forward primer	Reverse primer
Rat *Mmp9* (HSC)	5′-CAGACCAAGGGTACAGCCTGTT-3′	5′-AGCGCATGGCCGAACTC-3′
Rat *Mmp13*	5′-GCCCTATCCCTTGATGCCATT-3′	5′-ACAGTTCAGGCTCAACCTG-3′
Rat *Hdac1*	5′-AGGGCACCAAGAGGAAAGTCTGTT-3′	5′-AGTCATTCGGATTCGGTGAGGCTT-3′
Rat *Hdac2*	5′-TGGGCTGCTTCAACCTAACTGTCA-3′	5′-CCAAGCATCAGCAACGGCAAGTTA-3′
Rat *Hdac3*	5′-CATGACATGTGCCGCTTCCATTCT-3′	5′-AGGCTCTTGGTGAAACCCTGCATA-3′
Rat *Hdac4*	5′-AGGTGAAGATGAAGCTGCAGGAGT-3′	5′-TGTGCTGTGTCTTCCCATACCAGT-3′
Rat *Hdac5*	5′-TGAAATCCAGACCGTGCACTCTGA-3′	5′-TTACTGTCCAGCTTCTGCCGGTTA-3′
Rat *Hdac6*	5′-AACTCAGCTAACCAGACCACGTCA-3′	5′-GTCTGCTTGCTGGCATTTGAGGAT-3′
Rat *Gadph*	5′-CCTGGAGAAACCTGCCAAGTAT-3′	5′-CTCGGCCGCCTGCTT-3′
Mouse *Mmp13* (3T3)	5′-CTTCTGGTCTTCTGGCACACG-3′	5′-GGTAATGGCATCAAGGGATAGG-3′
Mouse *Hdac4*	5′-CTGGCATCCCTGTGTCATTTG-3′	5′-ACACAAGACCTGTGGTGAACCTT-3′
Mouse *Ctsb*	5′-GAAGAAGCTGTGTGGCACTG-3′	5′-GTTCGGTCAGAAATGGCTTC-3′
Mouse *Ctsc*	5′-CAACTGCACCTACCCTGATC-3′	5′-CTCGTCGTAGGCAGTATCCA-3′
Mouse *Ctsk*	5′-GGGCCAGGATGAAAGTTGTA-3′	5′-CACTGCTCTCTTCAGGGCTT-3′
Mouse *Ctsl*	5′-TCTCACGCTCAAGGCAATCA-3′	5′-AAGCAAAATCCATCAGGCCTC-3′
Mouse *CtsH*	5′-TCATGGCTGCAAAGGAGGT-3′	5′-TGTCTTCTTCCATGATGCCC-3′
Mouse *Gadph*	5′-GCACAGTCAAGGCCGAGAAT-3′	5′-GCCTTCTCCATGGTGGTGAA-3′
Human *Hdac4* (Cos7)	5′-AGTGGCCAGGTTATCAGTGG-3′	5′-GGAGAAGAGCCGAGTGTGTC-3′
Human *Gadph*	5′-CAGCCGAGCCACATCG-3′	5′-TGAGGCTGTTGTCATACTTCT-3′

HSC, hepatic stellate cell; qPCR, real-time quantitative PCR.

condition was performed in triplicate. Cycling conditions included hot activation (94°C for 2 minutes), amplification (95°C for 15 seconds, 60°C for 1 minute) repeated 40 times, and quantification by SYBR Green fluorescence measurement. The primers for quantitative RT-PCR are listed in Table 2.

Western Blot Analysis

For the cells embedded in 3D ECM, collagen lattices were collapsed by centrifugation at 5000 × *g* for 5 minutes at 4°C, and the pellets were collected. Then, 0.1 mL of SDS-PAGE sample buffer (62.5 mmol/L Tris-HCl of at 6.8, 2% SDS, 10% glycerol, 0.0025% bromophenol blue, and 0.1 mol/L dithiothreitol or 5% β-mercaptoethanol) was added to the wells to collect remaining cells, and then the lysate was transferred to the tubes containing gel pellets. The tubes were subjected to boiling for 5 minutes to dissolve the ECM complex. In some cases the lattices were digested by 500 μL of 0.5 mg/mL type I collagenase in phosphate-buffered saline (PBS) at 37°C for 20 minutes to free the cells from collagen. Collected cells were dissolved in 1× reducing sample buffer. Protein samples were resolved by SDS-PAGE, transferred to polyvinylidene difluoride membranes (Bio-Rad), and hybridized to appropriate primary antibodies and horseradish peroxidase–conjugated secondary antibodies for subsequent detection by enhanced chemiluminescence (p90719; Millipore, Billerica, MA).

Immunoprecipitation

For immunoprecipitation, 2 × 10^5 NIH/3T3 cells were embedded in 3D type I collagen. After 6 hours, cells were collected as previously described.[17] Whole-cell lysate (about 5 × 10^6 cells) was prepared in 1.0 mL of immunoprecipitation lysis buffer (50 mmol/L Tris-HCl at pH 7.6, 150 mmol/L NaCl, 1.0 mmol/L EDTA, 1.0% NP-40, 0.1% Na-deoxycholate, and 0.5% glycerol). The total lysate preparations were precleaned with 50 μL of Dynabeads Protein A slurry (InvitroGen) and incubated on a rotator for 30 minutes at 4°C. Then, 200 μg of whole-cell lysate was incubated with 5.0 μg of anti-HDAC4 antibody (Cell Signaling Technology) or normal rabbit IgG (Cell Signaling Technology) as a negative control, overnight at 4°C under rotation. Dynabeads Protein A slurry (30 μL) was added to pull down the immune complex at 4°C for 2 hours. Beads were collected with DynaMag magnets and washed three times with 500 μL 1× immunoprecipitation lysis buffer, and the proteins were released by boiling with 1× SDS-PAGE loading buffer and subjected to Western blot analysis for CtsH and HDAC4.

Cellular Fractionation

Nuclear and cytoplasmic protein fractionations were separated using a Beyotime Nuclear and Cytoplasmic Protein Extraction Kit (Beyotime Institute of Biotechnology, Jiangsu, China) according to the manufacturer's instructions. Briefly, about 5.0 × 10^5 NIH/3T3 cells were embedded in 3D gel in 24-well plates or seeded on plastic wells. After 24 hours, 3D gel lattice was dissolved by 0.5 mg/mL collagenase (Sigma-Aldrich) at 37°C for 20 minutes, and the cells were collected at 5000 × *g* at 4°C for 10 minutes. Then, the cytoplasmic proteins were prepared in cytoplasmic lysis buffer and the nuclear protein was isolated with nuclear extraction buffer. Protein concentration was measured using the Pierce BCA Protein Assay Kit (Pierce, Rockford, IL). Fractionation was determined by Western blot analysis.

In Vitro Degradation

CtsH and CtsL were activated according to the manufacturer's instructions (R&D Systems). HDAC4-His as substrate was prepared from lentiviral-transfected 293T cells and purified by nickel−nitrilotriacetic acid magnetic beads (Thermo Fisher, Claremont, CA). HDAC4-His was mixed with CtsH or CtsL in varying amounts in the following 50-μL reactions: 3 μL of HDAC4-His, 1 μL (26 μg) of bovine serum albumin, 2.5 μL of dithiothreitol (100 mmol/L), 47.5 μL of Tris buffer (100 mmol/L NaCl, 50 mmol/L Tris at pH 7.0, or 50 mmol/L HAc was used for pH 4.0 to 6.0). After incubation at 37°C for 2 hours, the reactions were resolved by Western blot analysis against HDAC4, CtsH, and CtsL.

Immunofluorescence Staining and Confocal Microscopy

Liver tissues were snap-frozen in liquid nitrogen and embedded in OCT compound. Sections of 5-μm thickness were fixed in ice-cold acetone for 10 minutes. Cell cultures on plastic and in 3D ECM were fixed with 4% paraformaldehyde in PBS for 10 minutes at room temperature. After three washes with PBS, cells were treated with 0.15% Triton X-100 in PBS for 10 minutes. Then the cells were blocked with 5% donkey serum in PBS and further incubated with appropriate primary antibodies at 4°C overnight. The following types and dilutions of primary antibodies were used: anti α−smooth muscle actin (1:200; Abcam, Cambridge, MA), anti-phalloidin (1:200; Abcam), anti-HDAC4 (1:200; Cell Signaling Technology), anti-HDAC7 (1:200; Cell Signaling Technology), and anti-CtsH (1:100; Santa Cruz Biotechnology, Dallas, TX). Slides were washed with PBS three times and then appropriate secondary fluorescent antibodies were added at 1:400 dilutions for 1 hour at room temperature. Nuclei were visualized with DAPI (Sigma-Aldrich). Immunofluorescence images were acquired using a Leica TC SP5 II confocal microscope equipped with a digital camera (Leica Microsystems, Wetzlar, Germany).

Statistical Analysis

Data were analyzed using Prism software version 6 (GraphPad Software, San Diego, CA). Statistical significance was determined using unpaired two-tailed *t*-test unless otherwise indicated, and $P < 0.05$ was considered significant. Numeric data are presented as means ± SEM.

Results

Stabilization of Class IIa HDAC Proteins during *Trans*-Differentiation of Hepatic Stellate Cells

We have previously shown that the MMP genes in the MMP locus on chromosome 8 (eg, *MMP3*, *MMP10*, *MMP13*) and *MMP9* on chromosome 3 are progressively suppressed/silenced during HSC *trans*-differentiation.[4,8] We reasoned that the suppression/silencing of MMP genes in myofibroblastic HSCs is likely mediated through epigenetic regulation. Cultured on plastic dish for up to 9 days, the rat qHSCs gradually acquired an activated phenotype and transformed into myofibroblast-like cells characterized by stress actin filaments and contraction (Figure 1A), and increased expression of α−smooth muscle actin (Figure 1B). The protein levels of class I HDACs, including HDAC1 and HDAC2, were not significantly changed during HSC *trans*-differentiation (Figure 1B). In contrast, HDAC4, a class IIa HDAC, was minimally expressed or barely detected in the qHSCs, whereas the fragmentations, as measured by antibodies against the N-terminus, were apparent (Figure 1B). After 9 days of culture activation on plastic, the full-length (140 kDa) HDAC4 was progressively accumulated, whereas the N-terminal fragments were concurrently diminished. Other class IIa HDACs, such as HDAC5, were weakly expressed in the HSCs, but exhibited a similar pattern of stabilization during HSC *trans*-differentiation (Figure 1B). Importantly, the mRNA levels of these HDACs did not change significantly during the course of *trans*-differentiation (Figure 1C), implying a potential mechanism of post-transcriptional regulation. Interestingly, we noted that in HSCs a protein band (about 250 kDa) (Figure 1B) migrated much slower than did HDAC4 protein but could still be recognized by HDAC4 antibody. We thought this protein band may be the modified and conjugated HDAC4 protein. Indeed we found these bands can also be recognized by small ubiquitin-like modifier (SUMO)-1 antibody (Supplemental Figure S1), indicating the involvement of SUMOylation in HDAC4 modification and also the complex mechanism of HDAC4 regulation at the protein levels.

By chromatin immunoprecipitation analysis we found that HDAC4 and -5 increasingly occupied in the 5′-promoter of *MMP9/13* (L.Q.),[8] which is in agreement with our previous work showing impaired histone acetylation and inaccessibility in the 5′-promoters of *MMP9* and -*MMP13*.[4,8] These results suggest that the accumulation of class IIa HDACs during *trans*-differentiation is through stabilization of their proteins, presumably through down-regulation of the putative HDAC-IIa degrading enzyme(s).

Levels of Proteins but Not mRNAs of the Class IIa HDACs Are Promptly Down-Regulated in qHSCs Embedded in 3D ECM

Next, we determined whether class IIa HDACs are down-regulated in the qHSCs grown in 3D ECM and whether this event is involved in de-repression of the MMP expression. Freshly isolated HSCs placed in 3D ECM maintained quiescent phenotypes, showing vitamin A droplets around their nuclei and p21 expression and cell cycle arrest at G_0 phase (data not shown and Figure 2A). In contrast, the HSCs seeded on plastic underwent spontaneous *trans*-differentiation, resulting in myofibroblastic phenotype,

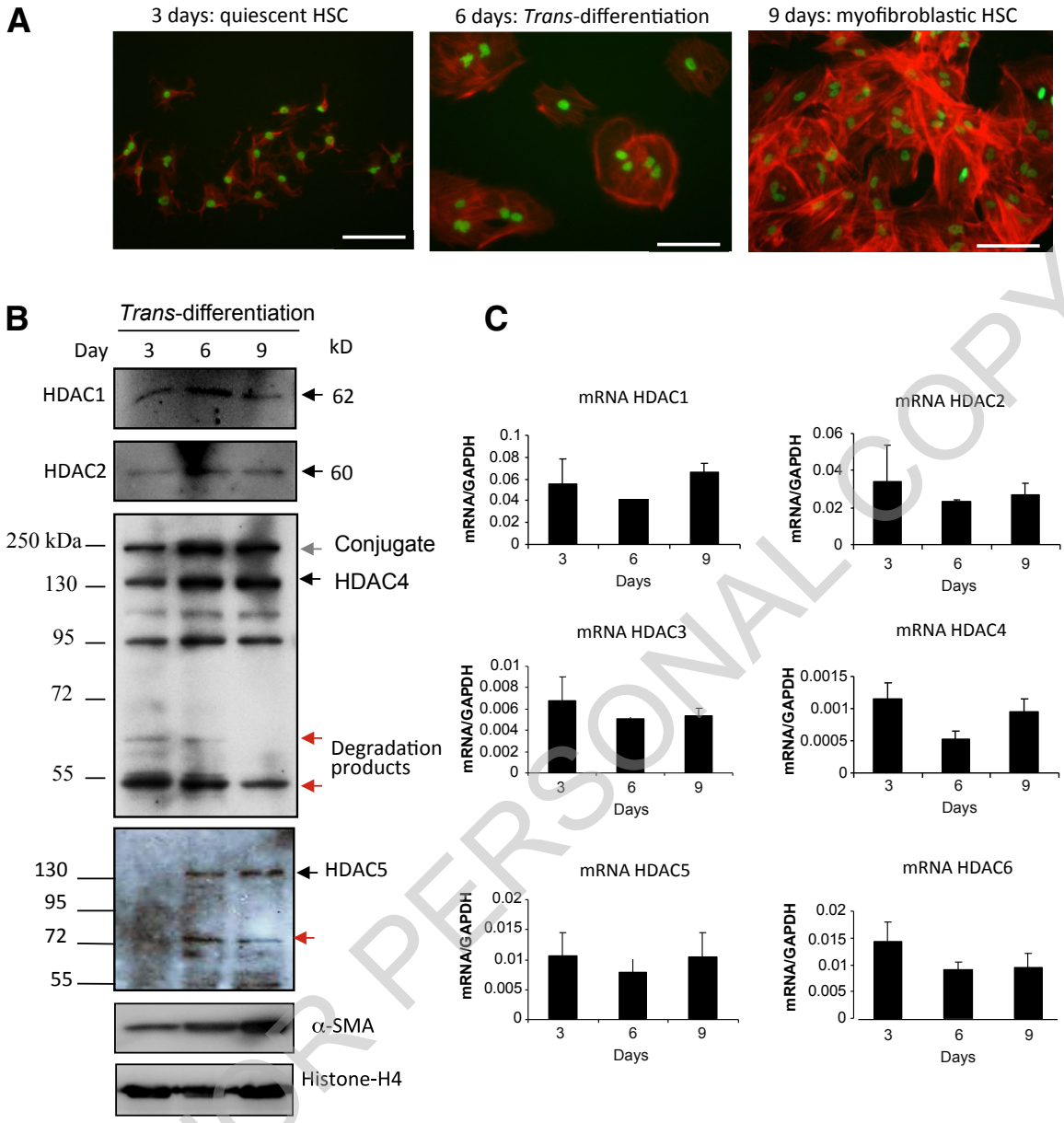

Figure 1 Class IIa histone deacetylase (HDAC) proteins, but not their mRNA levels, are up-regulated/stabilized in the course of hepatic stellate cell (HSC) *trans*-differentiation. **A:** *Trans*-differentiation of rat HSCs by culture activation is illustrated by phalloidin-Cy3 (red) staining of the HSCs cultured for 3, 6, and 9 days. **B:** Western blot analysis for class I HDACs (HDAC1 and HDAC2) and class IIa HDACs (HDAC4 and HDAC5) by HSCs cultured on plastic in the time course of *trans*-differentiation. The full-length HDACs are indicated with **black arrows**, a potential conjugated HDAC4 high-molecular band is indicated by the **gray arrow**, and the N-terminal fragments, being recognized by the antibodies, are indicated by **red arrows. C:** The mRNA levels of the HDACs by the HSCs in *trans*-differentiation stages were determined by real-time quantitative RT-PCR analysis. All of the experiments were performed at least three times, and representative images are shown. Data are expressed as means ± SEM. Scale bars = 20 μm. GAPDH, glyceraldehyde-3-phosphate dehydrogenase; SMA, smooth muscle actin.

indicated by loss of vitamin A droplets and the formation of conspicuous actin filaments (Figure 2A). Remarkably, the HDAC4 and HDAC7 proteins vanished in the qHSCs embedded in the 3D ECM gel, but markedly increased in the HSCs cultured on plastic (Figure 2B). Also, in the 3D ECM gel but not on the plastic culture, the HSCs acquired the ability to express *MMP9* and *MMP13* on IL-1β challenge (Figure 2C).

We noted that other cells of mesenchymal origin, such as the NIH/3T3 fibroblasts, exhibited quiescent phenotypes similar to those of the HSCs when the cells were cultured in 3D ECM gel, showing the morphologic cytoplasmic extension, cell cycle arrest in G_0, and the ability to express *MMP13* and other MMP genes on TNF-α stimulation (Figure 2, D–F).[17] Likewise, in 3D ECM culture, there was marked down-regulation of HDAC4, but not of class I HDACs, in NIH/3T3 cells (Figure 2G). Overexpression of HDAC4 in these cells suppressed TNF-α–initiated expression of *MMP13* (Figure 2, H and I). These results suggest that down-regulation of class IIa HDACs may contribute to

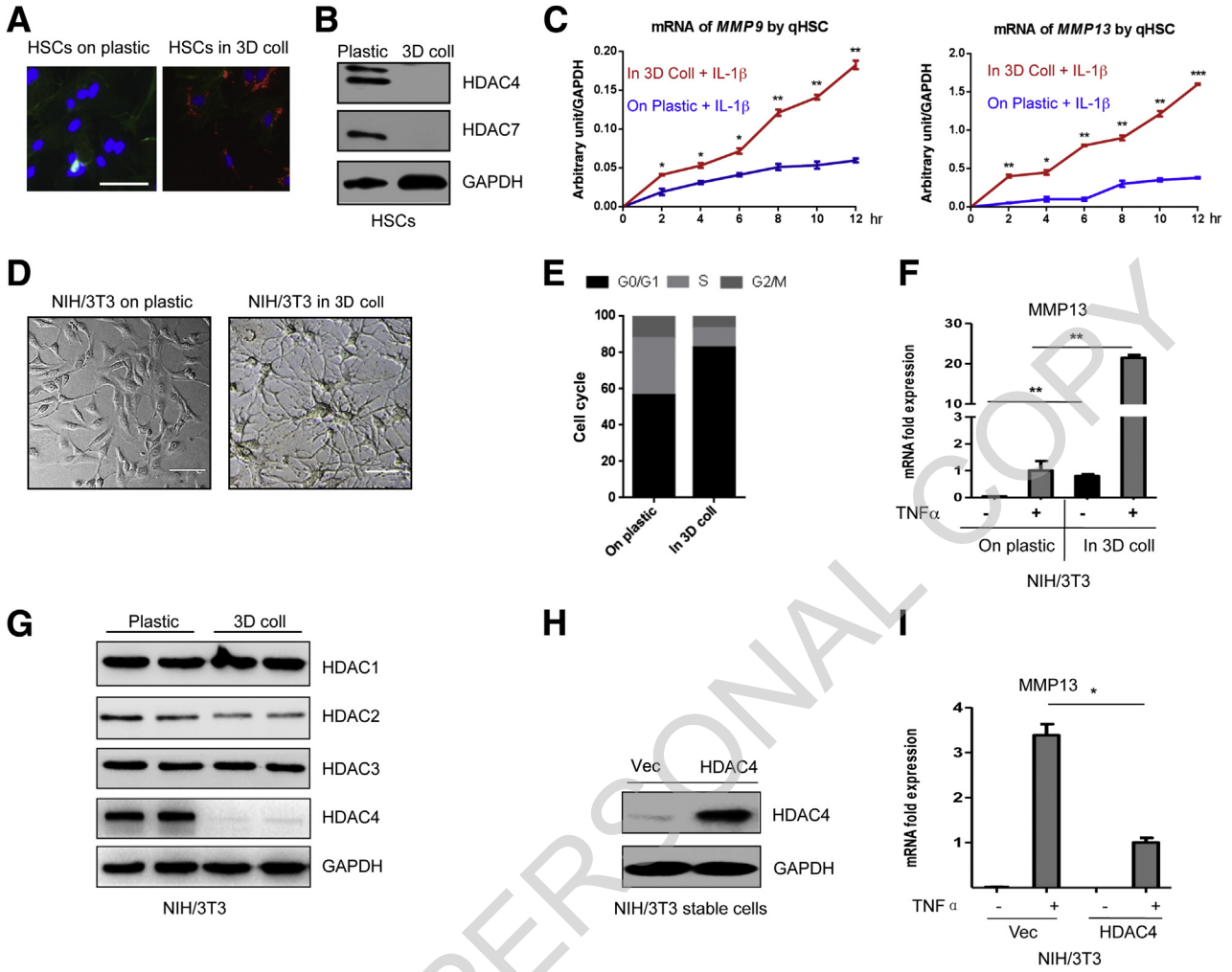

Figure 2 In three-dimensional extracellular matrix (3D ECM), class IIa histone deacetylases (HDACs) are promptly down-regulated, which confers the matrix metalloproteinase (MMP) genes into a permissive state. **A:** Isolated rat hepatic stellate cells (HSCs) were seeded on plastic or embedded in 3D type I collagen. After culturing for 9 days, the cells were stained for α—smooth muscle actin (green) by immunofluorescence staining; nuclei were marked by DAPI (blue). The peripheral vitamin A droplets (red) were autofluorescent under UV light. **B:** Western blot analysis of class IIa HDACs by the HSCs cultured on plastic or in 3D ECM. **C:** The quiescent (q) HSCs were seeded on plastic or embedded in 3D collagen, followed by IL-1β stimulation for the indicated periods. Expression levels of *MMP9* and *MMP13* were determined by real-time quantitative RT-PCR analysis. **D:** The phenotypes of NIH/3T3 cells, grown on plastic or in 3D collagen, were imaged by phase contrast microscopy. **E:** Fluorescence-activated cell sorting analysis of the cell-cycle distribution by which the NIH/3T3 cells were cultured in 3D collagen and on plastic for 48 hours. **F:** Expression of *MMP13* by NIH/3T3 cells in the two culture types in response to tumor necrosis factor (TNF)-α stimulation by real-time quantitative RT-PCR. **G:** Expression of HDACs by NIH/3T3 cells cultured on plastic or in 3D collagen as determined by Western blot analysis. **H:** Overexpression of HDAC4 in NIH/3T3 cells was determined by Western blot analysis. **I:** Impact of exogenous HDAC4 on *MMP13* gene expression induced by TNF-α, as determined by real-time quantitative RT-PCR analysis. All experiments were performed at least twice, and representative images are shown. For the mRNA measurement by real-time quantitative RT-PCR analysis, triplicated wells were applied for each condition, and glyceraldehyde-3-phosphate dehydrogenase (GAPDH) was selected as the internal control. Data are expressed as means ± SEM. $*P < 0.05$, $**P < 0.01$, and $***P < 0.001$. Scale bars = 20 μm. coll, collagen 1; vec, vector.

the permissive state for the mesenchymal cells in soft 3D ECM, and that up-regulation of class IIa HDACs is related to the nonpermissive state for MMP suppression/silencing in fibrosis.

Cysteine Cathepsins Mediate HDAC4 Degradation

We considered that a common epigenetic mechanism might exist in mesenchymal cells other than HSCs. We then addressed how HDAC4 was down-regulated in mesenchymal cells under the 3D ECM culturing condition. As shown with NIH/3T3 cells, the HDAC4 protein levels were predominantly down-regulated at 24 hours after embedding in the 3D collagen gel, whereas the mRNA levels were largely unchanged (Figure 3, A and B). To exclude potential translational silencing or suppression, which relies on the untranslated regions in its transcript, we also generated a FLAG-HDAC4 fusion construct without the 5′ or 3′ untranslated region elements of the *HDAC4* gene. When overexpressed in NIH/3T3 cells, the levels of

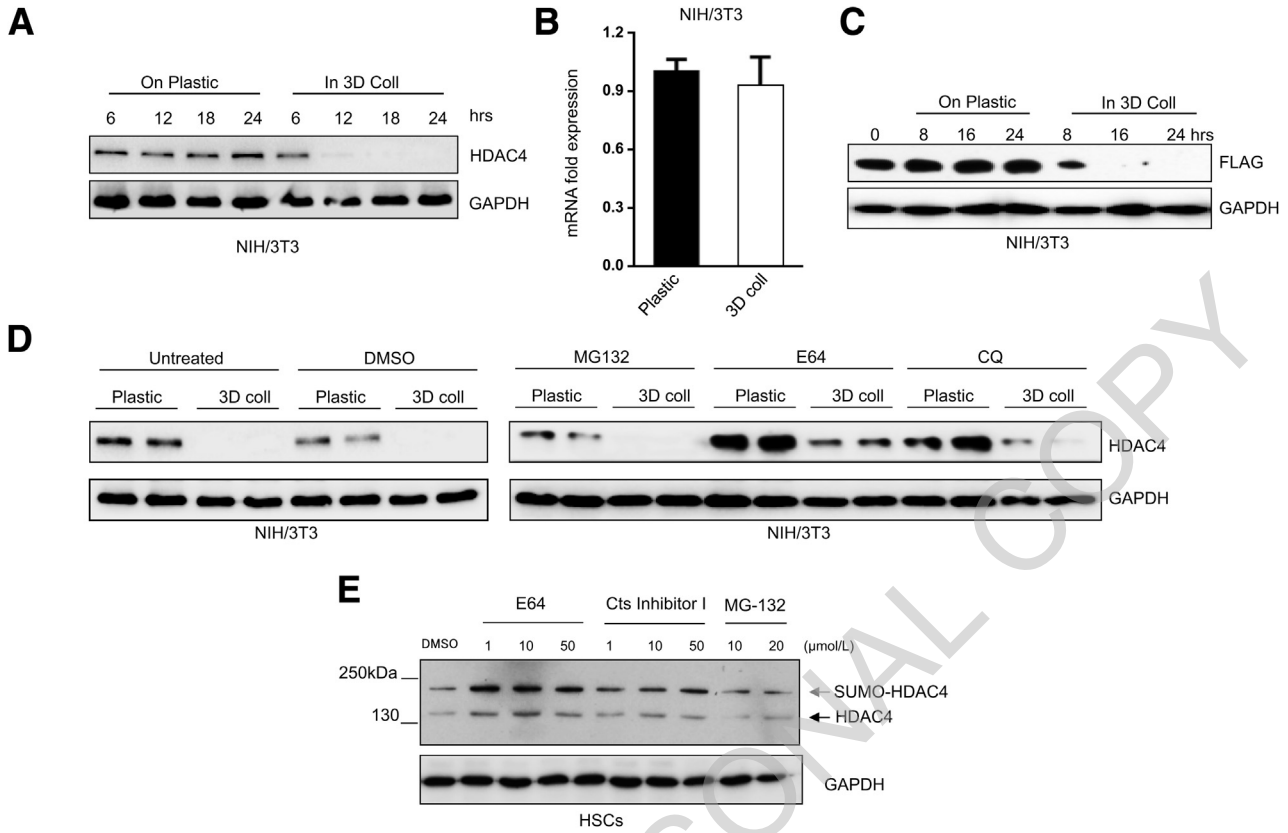

Figure 3 Turnover of histone deacetylases (HDAC)-4 is blocked by inhibitors of cysteine cathepsins. **A:** NIH/3T3 cells were seeded on plastic or embedded in 3D collagen for 6, 12, 18, and 24 hours. Levels of HDAC4 and glyceraldehyde-3-phosphate dehydrogenase (GAPDH) were determined by Western blot analysis. **B:** The mRNA levels of *HDAC4* by NIH/3T3 cells cultured on plastic or in three-dimensional (3D) collagen for 24 hours were determined by real-time quantitative RT-PCR analysis. **C:** Exogenous FLAG-HDAC4, driven by cytomegalovirus promoter, was expressed in NIH/3T3 cells. The resulting cells were then seeded on plastic or embedded in 3D collagen for indicated interval followed by Western blot analysis for HDAC4 and GAPDH. **D:** NIH/3T3 cells were seeded on plastic or embedded in 3D collagen, followed by 12-hour treatment with MG132 for proteasome (20 and 40 μmol/L), E64 (20 and 50 μmol/L) for cysteine proteinases, and chloroquine (CQ; 50 and 100 μmol/L) for acid proteinases. The levels of HDAC4 and GAPDH proteins were determined by Western blot analysis. **E:** Rat primary hepatic stellate cells (HSCs) at quiescent state were treated with E64, cathepsin inhibitor I, and MG132 at the indicated concentrations for 4 hours. The protein levels of HDAC4 and GAPDH were determined by Western blot analysis. Experiments were performed at least three times and representative images are shown. For the mRNA measurement by real-time quantitative RT-PCR analysis, triplicated wells were applied for each condition, the experiments were repeated at least twice, and GAPDH was selected as the internal control. Data are expressed as means ± SEM. coll, collagen; Cts, cathepsin; DMSO, dimethyl sulfoxide; SUMO, small ubiquitin-like modifier.

the FLAG-HDAC4 protein started to reduce after the cells were embedded in 3D ECM for 6 hours, and the protein totally vanished within 12 hours by the cells in 3D ECM (Figure 3C). These results further suggest that down-regulation of HDAC4 is mediated through protein degradation, rather than transcriptional or translational suppression.

To identify the protease activity involved in the degradation of HDAC4, we first determined whether treatment with proteinase inhibitors could restore the lost HDAC4 by NIH/3T3 cells cultured in 3D ECM. To our surprise, MG132, a specific inhibitor of proteasome, did not rescue the loss of HDAC4 protein in the 3D collagen culture, whereas p21, a known substrate of the proteasome pathway, was significantly greater (Figure 3D and data not shown). Second, chloroquine, which inhibits cysteine cathepsin activities by raising intracellular pH, partially rescued the HDAC4 by the cells cultured either on plastic or in 3D ECM. Third, E64, an inhibitor of cysteine proteinases, also partially restored the HDAC4 levels by the cells embedded in 3D ECM (Figure 3D). Similar results were observed in the qHSCs, in which two inhibitors of cysteine cathepsin (E64 and CtsL inhibitor I), but not MG132, promptly restored HDAC4 protein in 4 hours of treatment (Figure 3E). Taken together, these findings strongly indicate that cysteine-type cathepsins, but not the general ubiquitin proteasome pathway, are likely involved in HDAC4 degradation in mesenchymal cells including the qHSCs.

Cysteine-Type Cathepsins Are Up-Regulated in Cells Cultured in 3D ECM, but Down-Regulated during HSC *Trans*-Differentiation to Myofibroblasts

Through Affymetrix DNA microarray analysis we profiled the expression patterns of the cysteine-type cathepsins in

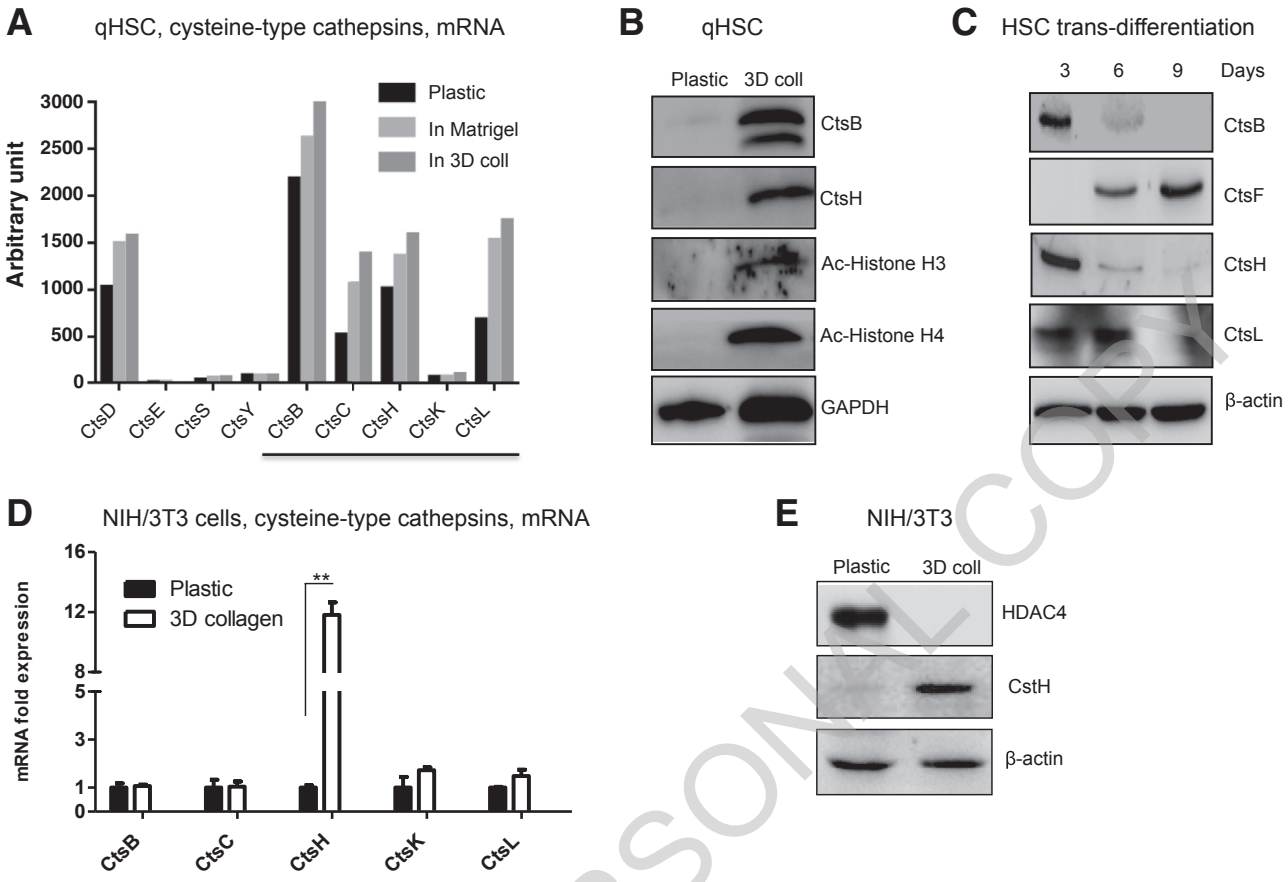

Figure 4 Up-regulation of cysteine cathepsins (Cts) by the cells in three-dimensional extracellular matrix (3D ECM) is associated with down-regulation of histone deacetylase (HDAC)-4; and conversely, down-regulation of the cathepsins in the hepatic stellate cells (HSCs) during *trans*-differentiation is linked to stabilization of HDAC4. **A:** Expression of cathepsins by quiescent (q) HSCs cultured on plastic or embedded in 3D ECM (type I collagen and Matrigel) was determined by DNA microarray analysis. The cysteine-type cathepsins are indicated by a bar. **B:** The protein levels of two cysteine cathepsins and the N-terminal acetylated histones H3 and H4 by qHSCs seeded on plastic or embedded in 3D collagen were determined by Western blot analysis. **C:** The cysteine cathepsins related to HSC *trans*-differentiation were determined by Western blot analysis. **D:** 3D collagen—mediated elevation of cysteine cathepsins at the mRNA level in NIH/3T3 cells as determined by real-time quantitative RT-PCR analysis. **E:** The inverse association between CtsH elevation and HDAC4 down-regulation by NIH/3T3 cells in 3D collagen as determined by Western blot analysis. All experiments were performed at least twice, and representative images are shown. Data are expressed as means ± SEM (**D**). $^{**}P < 0.01$. coll, collagen; GAPDH, glyceraldehyde-3-phosphate dehydrogenase.

qHSCs cultured on plastic versus embedded in type I collagen or in Matrigel. Firstly, the mRNA levels of cysteine-type cathepsins, including CtsB, CtsC, CtsH, and CtsL, were highly expressed in qHSCs (Figure 4A). Importantly, the levels of expression of these cysteine-type cathepsins were all further enhanced by the cultures in 3D ECM. Second, the protein levels of CtsB and -H, as determined by Western blot analysis, were substantially up-regulated in the qHSCs grown in 3D ECM, but were barely detected in the culture on plastic (Figure 4B). Third, in agreement with the elevation of these cathepsins in the 3D ECM culture, the protein levels of class IIa HDACs, including HDAC4 and -7 (Figure 2B), were markedly decreased, leading to elevation of histone acetylation (Figure 4B). Therefore, the cysteine-type cathepsins fit well with our anticipated criteria of being potential HDAC4 degrading enzymes, which are not only present but also up-regulated in the HSCs in the permissive state.

Conversely, we further anticipated that in the nonpermissive state, such as myofibroblastic HSCs, there would be an opposite pattern, showing down-regulation of the cathepsins and up-regulation of class IIa HDACs. The protein levels of CtsB, CtsH, and CtsL were progressively down-regulated in the course of HSC *trans*-differentiation (Figure 4C), and totally diminished in the end stage of myofibroblastic HSCs (Figure 1B). Of importance is that the down-regulation of cysteine-type cathepsins is in agreement with the stabilization/accumulation of HDAC4, suggesting a potential causal link.

Moreover, we anticipated a common mechanism for the regulation of class IIa HDACs for other mesenchymal cells. In this regard, we further examined the inverse association between increased cysteine cathepsins and degradation of HDAC4 in NIH/3T3 fibroblasts. These cells were seeded on plastic or imbedded in 3D type I collagen for 24 hours. The expression of cysteine cathepsins was determined by real-

time quantitative RT-PCR analysis. The *CtsH* expression was elevated 12-fold by the cells embedded in 3D ECM in comparison with that by culture on plastic (Figure 4D). Western blot analysis demonstrated a tight inverse association between the increased *CtsH* and down-regulation of HDAC4 by the cells in 3D ECM (Figure 4E), further suggesting that cysteine-type cathepsins are HDAC4-degrading enzymes.

Catalytic Function of CtsH Is Required for HDAC4 Degradation in the Cells

To directly test cathepsin-dependent degradation of HDAC4, we performed a cotransfection experiment in Cos7 cells with plasmids expressing CtsH and HDAC4 with a His tag at the C-terminus (Figure 5A). The levels of HDAC4 were determined by Western blot analysis after 24 hours of transfection. Apparently degraded products of HDAC4, in the range of 90 to 50 kDa, were detected by antibodies against the N-terminus of HDAC4, showing dose-dependent fragmentation with increased CtsH expression. The endogenous full-length HDAC4 (which, at 140 kDa, has a molecular weight slightly lower than that of the His-tagged variant) promptly decreased in response to the increased expression of CtsH. However, the exogenously expressed HDAC4-His, as driven by a cytomegalovirus promoter for its expression, was steadily generated. Western blot analysis with anti-His antibody produced complementary results, showing CtsH-dependent fragmentation of HDAC4, as measured by the C-terminal tag (Figure 5A). Furthermore, the matured CtsH at 25 kDa and its precursor at 40 kDa were evidently increased along with the scale of HDAC4 degradation, whereas the level of glyceraldehyde-3-phosphate dehydrogenase, an internal control, was not altered. We then extended our examination to include other mesenchymal cells such as NIH/3T3 and HEK-293, and we confirmed that ectopic expression of CtsH could effectively down-regulate the endogenous HDAC4 (Figure 5B). To further define the role of the proteolytic activity of CtsH, we generated an enzymatically deficient variant by replacing

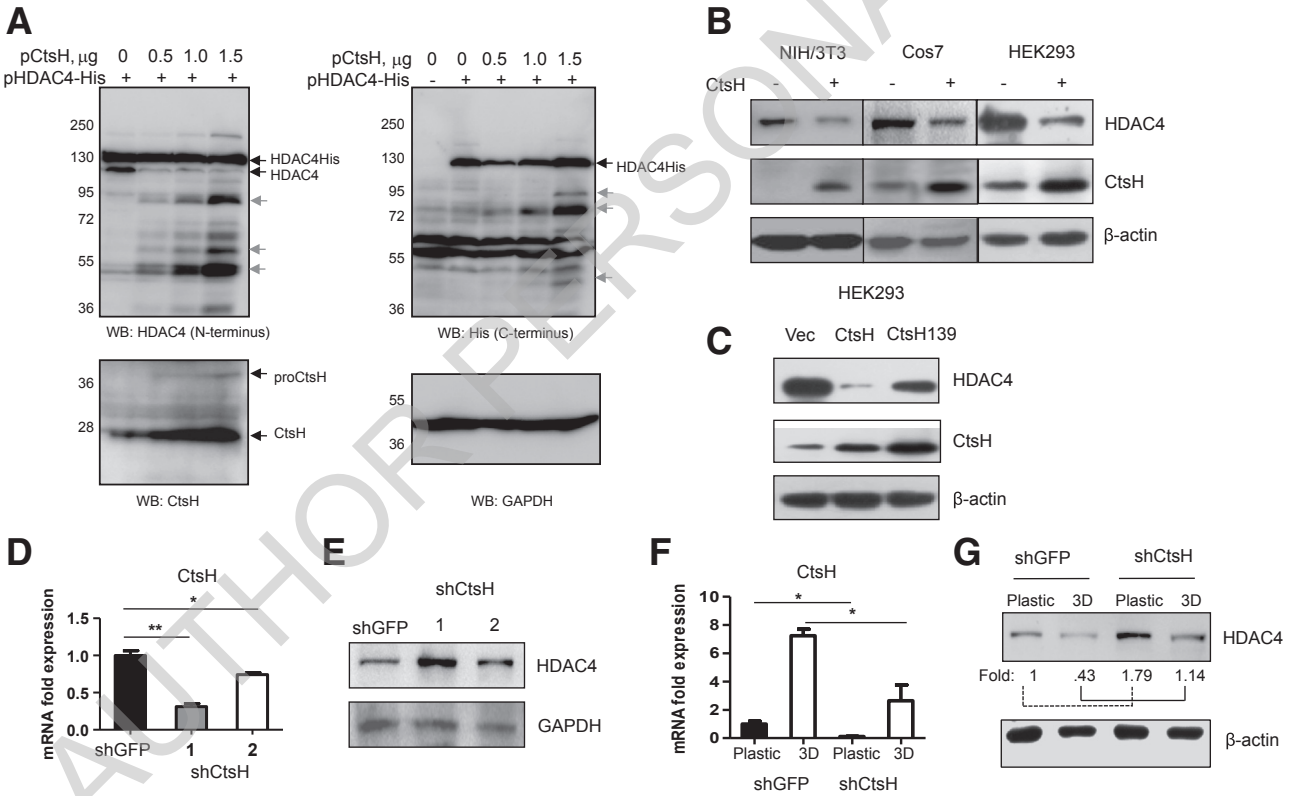

Figure 5 Cathepsin (Cts) H-mediated degradation of histone deacetylase (HDAC)-4 in cells. **A:** Cos7 cells were cotransfected with plasmids to express HDAC4-His as a substrate, together with an increased dose of CtsH as a potential degradation enzyme. HDAC4 and its degradation products were recognized in Western blot (WB) through antibodies against the N-terminal domain or C-terminal His tag. The endogenous HDAC4, which migrated slightly faster, and the extraneous HDAC4-His variant are indicated with **black arrows**. The potential degradation products of HDAC4 are indicated by **gray arrows**. **B:** NIH/3T3, Cos7, and HEK-293 cells were transfected with a plasmid expressing CtsH. The levels of endogenous HDAC4 were determined by Western blot analysis. **C:** A catalytic dead CtsH variant (Cys139Ser) and the wild type were expressed in HEK-293 cells. The down-regulation of HDAC4 was determined by Western blot analysis. **D:** Lentiviral vector (vec) was used for delivering shRNA to knock down *CtsH* by the cells cultured on plastic, and the efficiency of knockdown was measured by real-time quantitative RT-PCR analysis. **E:** The effect of *CtsH* knockdown on HDAC4 protein level was measured by Western blot analysis. **F** and **G:** Knockdown of endogenous *CtsH* in HEK-293 cells cultured in three-dimensional (3D) collagen partially restores the HDAC4, as determined by real-time quantitative RT-PCR and Western blot analysis, respectively. Data are expressed as means ± SEM. n = 3 independent experiments. $*P < 0.05$, $**P < 0.01$. GAPDH, glyceraldehyde-3-phosphate dehydrogenase; GFP, Green fluorescent protein.

Cys139, a major catalytic residue for cysteine cathepsins. As anticipated, the catalytically dead variant of CtsH lost its ability to down-regulate HDAC4 in the cells (Figure 5C).

In an RNA-interference experiment, we used a lentiviral vector to deliver shRNA targeting the mRNA of *CtsH* or green fluorescent protein. Partial knockdown of *CtsH* resulted in increased HDAC4 protein levels (Figure 5, D and E). Because CtsH was substantially up-regulated in the 3D ECM culture, we tested whether knockdown of the endogenous *CtsH* in 3D culture could rescue the loss of HDAC4. HDAC4 was elevated moderately by the NIH/3T3 cells cultured either on plastic or in 3D collagen, in line with the extent of *CtsH* knockdown (Figure 5, F and G).

CtsH and CtsL Can Directly Digest HDAC4 *in Vitro*

Recombinant human CtsH and CtsL were used for *in vitro* degradation analysis. The reactions were performed through incubation of the purified HDAC4-His with the activated CtsH protein in various doses at pHs 4 and 7. After 2-hour incubation, the degradation products were analyzed by Western blot. HDAC4 was degraded completely by CtsH at acidic pH, and partially at neutral pH (Figure 6A). Similarly, CtsL also digested HDAC4 at acidic pH (Figure 6, B and C). These results are consistent with the finding of inhibition of cysteine-type cathepsins by the specific proteinase inhibitors or chloroquine, which raises the subcellular pH, resulting in increased HDAC4 protein levels (Figure 3D), further suggesting that certain acidic cysteine-type cathepsins are involved in HDAC4 degradation.

Subcellular Localization and Physical Association between CtsH and HDAC4

We further extended our study to address how the cysteine-type cathepsins, which are known to be located primarily in lysosome, could mediate HDAC4 degradation. HDAC4, among other members of class IIa HDACs, was known to be shuttling between the nucleus and the cytoplasm.[18] First, through confocal microscopy analysis, we examined the subcellular localizations of CtsH and HDAC4. The physical binding of CtsH and HDAC4 should be transient, with CtsH being the degrading enzyme and HDAC4 being the targeting substrate. To capture the transition state, we thus examined their subcellular localizations by the cells seeded for 6 hours on plastic or embedded in 3D collagen. For the condition of cultivation on plastic for 6 hours, CtsH protein was barely detectable in either the cytoplasmic or nuclear compartment (Figure 7A), whereas HDAC4 was present in both the cytoplasm and nuclei. In contrast, after culturing of the cells for 6 hours in 3D collagen, CtsH protein was drastically up-regulated and present in the cytoplasmic and nuclear compartments in the form of puncta, whereas HDAC4 was decreased in the cytoplasm and was essentially absent in the nuclei.

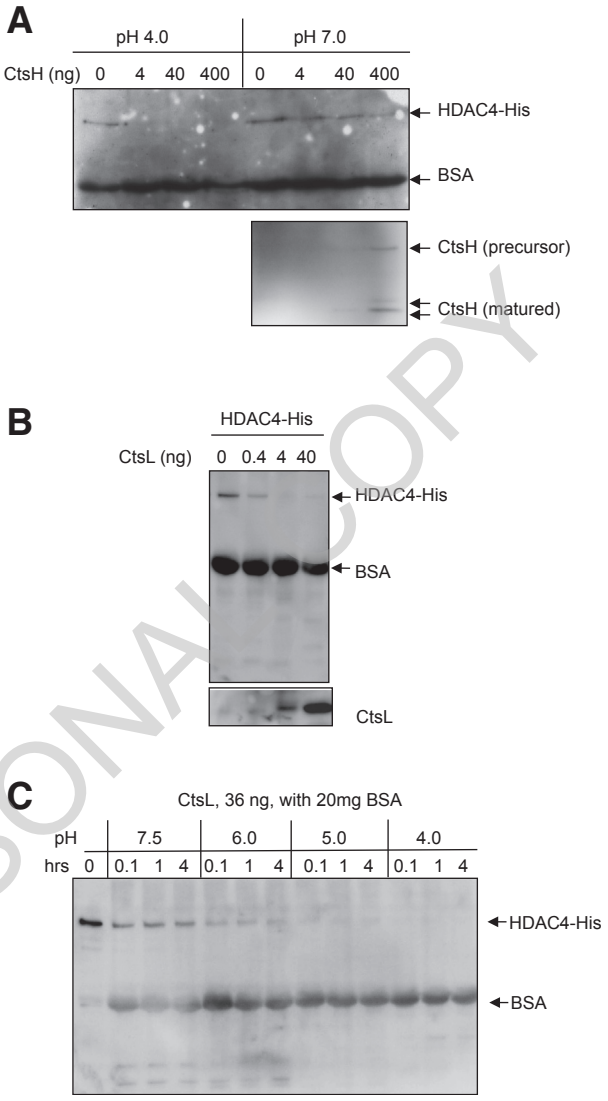

Figure 6 Cathepsin (Cts)-H directly degrades histone deacetylase (HDAC)-4 *in vitro*. **A:** Recombinant human CtsH and CtsL were activated to generate mature forms. The reactions were performed at two pH values by incubation of the purified HDAC4-His with CtsH in various doses for 2 hours. The reaction products were resolved by Western blot against HDAC4 and CtsH. **B:** Recombinant human CtsL and HDAC4-His were incubated in pH 4.5 buffer for 2 hours, and the degradation was monitored by Western blot analysis. **C:** The CtsL-mediated degradation of HDAC4-His at four pH values in a time course was monitored by Western blot analysis. The experiments were repeated twice and representative images are shown. BSA, bovine serum albumin.

Second, through cellular fractionation analysis, we measured the inverse pattern of subcellular distributions between CtsH and HDAC4 by the NIH/3T3 cells cultured in 3D collagen and on plastic. Cellular fractionation was successfully achieved, as indicated by histone H3 and lamin A/C for nuclear compartment and glyceraldehyde-3-phosphate dehydrogenase as a cytoplasmic protein marker (Figure 7B). When the cells were cultured on plastic, CtsH was expressed at very low levels, if at all, in all fractions, whereas HDAC4 was predominantly found in the

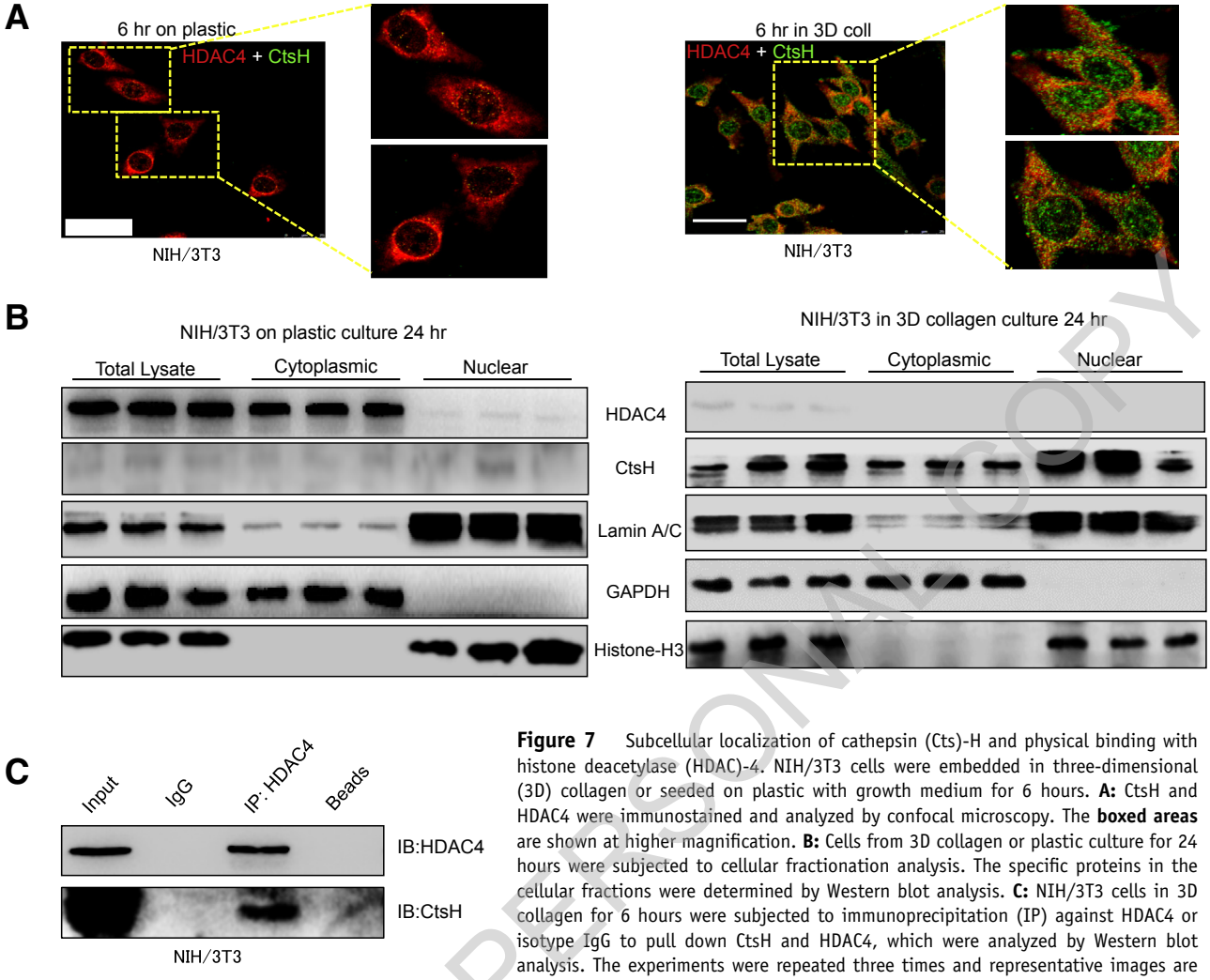

Figure 7 Subcellular localization of cathepsin (Cts)-H and physical binding with histone deacetylase (HDAC)-4. NIH/3T3 cells were embedded in three-dimensional (3D) collagen or seeded on plastic with growth medium for 6 hours. **A:** CtsH and HDAC4 were immunostained and analyzed by confocal microscopy. The **boxed areas** are shown at higher magnification. **B:** Cells from 3D collagen or plastic culture for 24 hours were subjected to cellular fractionation analysis. The specific proteins in the cellular fractions were determined by Western blot analysis. **C:** NIH/3T3 cells in 3D collagen for 6 hours were subjected to immunoprecipitation (IP) against HDAC4 or isotype IgG to pull down CtsH and HDAC4, which were analyzed by Western blot analysis. The experiments were repeated three times and representative images are shown. Scale bars = 25 μm. GAPDH, glyceraldehyde-3-phosphate dehydrogenase.

cytoplasmic fractions. Conversely, in 3D ECM culture, CtsH was profoundly increased in both the nuclear and cytoplasmic fractions, whereas HDAC4 was concurrently diminished.

Third, through immunoprecipitation analysis, we found that CtsH and HDAC4 formed a physical complex at 6 hours' transition time by the cells cultured in 3D collagen (Figure 7C). Taken together, these results demonstrate that HDAC4 is a potential substrate for CtsH-mediated degradation in the qHSCs and other mesenchymal cells in 3D ECM environment.

Degradation of HDAC4 May Occur in Both Nuclear and Cytoplasmic Compartments

To map the structural regions of HDAC4 that are involved in CtsH-mediated degradation, we generated a panel of truncated and site-mutated HDAC4 variants, which were tagged with an N-terminal FLAG epitope (Figure 8A). The NIH/3T3 cells were transfected with the plasmids, and the subcellular localization of the HDAC4 variants was determined by immunofluorescence staining against FLAG (Figure 8B). Similar to the endogenous HDAC4, the exogenous full-length FLAG-HDAC4 (wild type) was distributed in both nuclear and cytoplasmic compartments. The L1062A variant, in which a nuclear export signal was destroyed through replacement of the leucine-1062 with alanine, was exclusively located in nucleus. The N-terminal domain, containing the nuclear localization signal of 1-359 amino acid residues, was also found in the nucleus as expected. Instead, the C-terminal domain, containing the nuclear export signal, was mostly distributed in cytoplasmic compartment (Figure 8B). As measured by Western blot analysis, all of these variants were expressed in the cells cultured on plastic, but were promptly diminished in the cells embedded in 3D collagen (Figure 8, C and D).

We also examined the impact of the ectopically expressed CtsH on the wild-type FLAG-HDAC4 or the L1062A variant. The expression levels of both the L1062A variant and the wild type HDAC4 were reduced on coexpression of CtsH (Figure 8, E and F). Taken together, these results

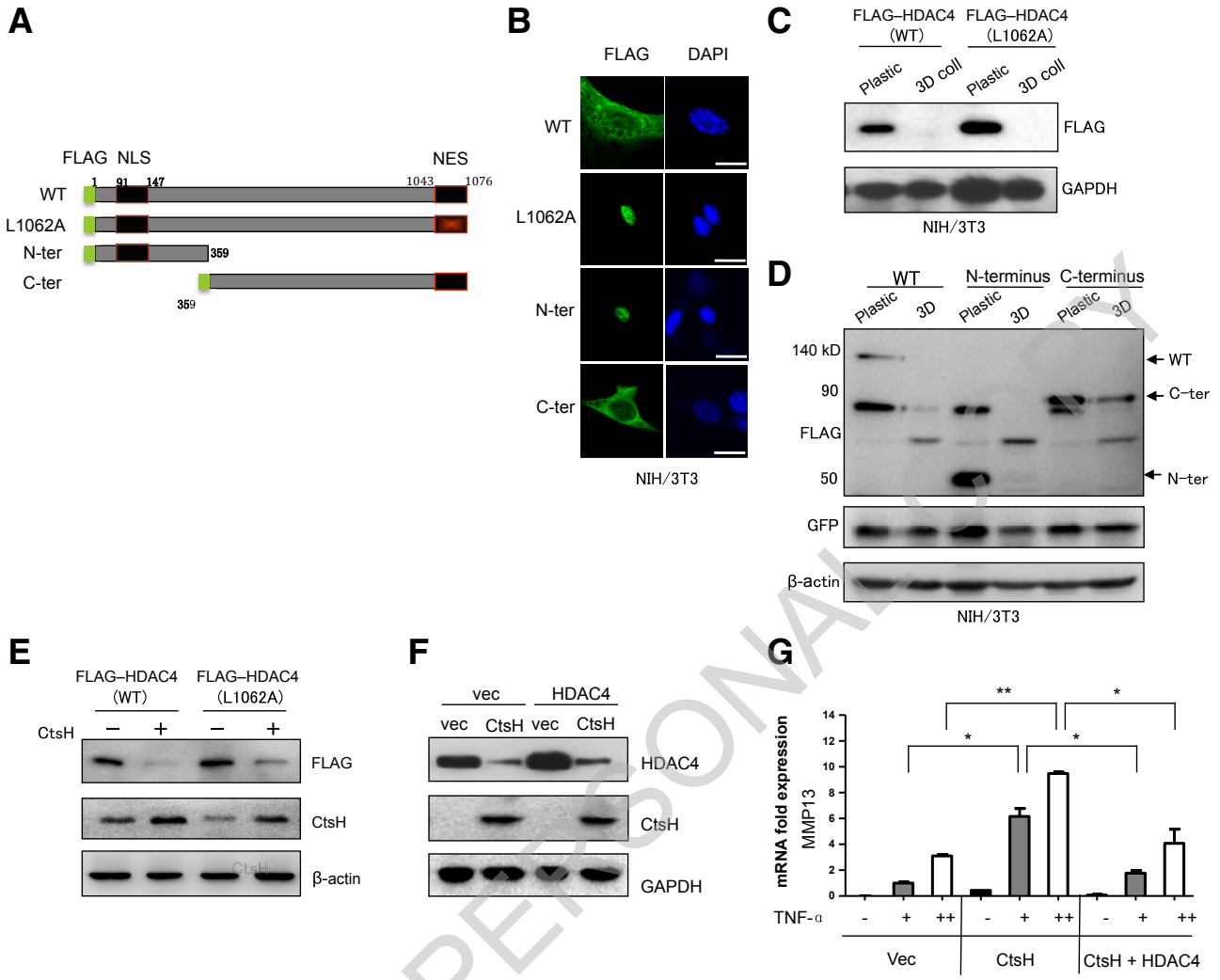

Figure 8 Histone deacetylase (HDAC)-4 degradation occurs in cytoplasmic and nuclear compartments. **A:** Schematic diagram of the HDAC4 variants: N-terminally (ter) FLAG-tagged full-length HDAC4 construction, nuclear localization signal (NLS), nuclear export signal (NES), and L1062A (the Leu 1062 in HDAC4 was replaced by Ala). **B:** NIH/3T3 cells were transfected with wild-type (WT) FLAG-HDAC4 or FLAG-HDAC4 variants, and the expression of the HDAC4 variants and their localization were measured through immunofluorescence staining (anti-FLAG staining in green). **C:** The stability of the HADC4 variants in the NIH/3T3 cells cultured on plastic or in three-dimensional (3D) collagen was measured by Western blot analysis against FLAG. **D** and **E:** Stability of wild-type FLAG-HDAC4 and L1062A mutant in NIH/3T3 cells cultured on plastic or embedded in 3D collagen together with overexpression of cathepsin (Cts)-H was measured by Western blot analysis. **F:** Overexpression of CtsH tagged with hemagglutinin-epitope in NIH/3T3 cells to induce degradation of endogenous HDAC4 was determined by Western blot analysis. **G:** The NIH/3T3 cells stably expressing CtsH and HDAC4 were embedded in 3D collagen and challenged with an increased concentration of tumor necrosis factor (TNF)-α. The expression of *MMP13* was determined by real-time quantitative RT-PCR analysis. All experiments were performed at least twice. Data are expressed as means ± SEM. $*P < 0.05$, $**P < 0.01$. Scale bars = 20 μm. coll, collagen; GAPDH, glyceraldehyde-3-phosphate dehydrogenase; GFP, green fluorescent protein; vec, vector.

suggest that both the N-terminal and the C-terminal regions of HDAC4 are liable to CtsH-mediated degradation in the 3D culturing condition and that the degradation can occur in both the cytoplasm and nucleus.

CtsH, through Down-Regulating HDAC4 in 3D ECM, Confers *MMP13* Gene into a Permissive State for TNF-α Stimulation

Given the current results of the CtsH-mediated degradation of HDAC4 and our previous work showing that HDAC4 suppresses MMP expression,[8] we determined whether overexpression of CtsH can reverse HDAC4 suppression of *MMP13* expression. Using a lentiviral expression system, we generated an NIH/3T3 cell line that stably expressed high levels of ectopic CtsH or HDAC4 (Figure 8G). As expected, we found that overexpression of CtsH could further enhance the expression of *MMP13* on TNF-α stimulation. In contrast, HDAC4 overexpression suppressed TNF-α–induced transcription of *MMP9/13*, suggesting that CtsH-mediated HDAC4 degradation in mesenchymal cells confers the MMP genes into an epigenetically permissive state.

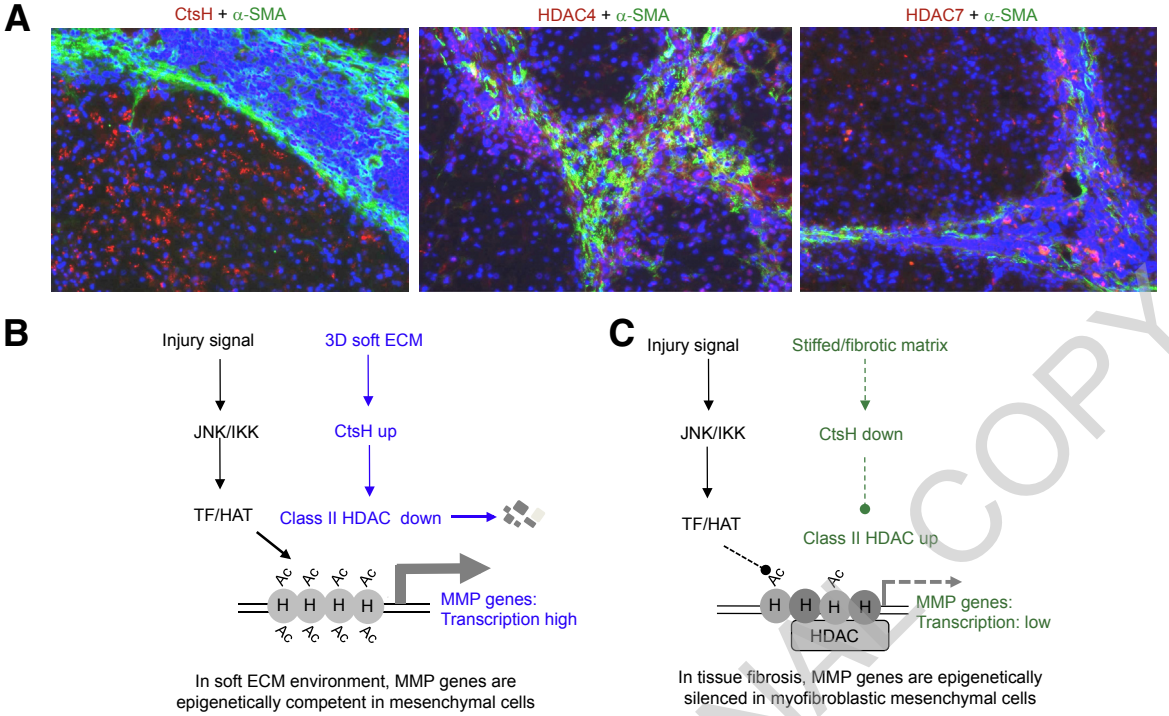

Figure 9 Elevation of class IIa histone deacetylases (HDACs) and down-regulation of cathepsin (CTS)-H in the fibrotic stroma of human cirrhotic liver and proposed working models. **A:** The human liver specimens, all derived from hepatitis C virus–mediated hepatocellular carcinoma, were analyzed by immunofluorescence staining, showing elevation of HDAC4 and -7 within the fibrotic septa. CtsH was mostly absent within the fibrotic septa, but presented in the parenchyma outside of fibrosis. **B** and **C:** Working models showing an underlying mechanism for a permissive state for matrix metalloproteinase (MMP) genes by mesenchymal cells, including quiescent hepatic stellate cells, in three-dimensional extracellular matrix (3D ECM). In particular, soft ECM can induce the expression of cysteine cathepsins, which consequently degrade the class IIa HDACs, conferring the cells into an epigenetically permissive state, as indicated by great power of MMP expression in response to injury signals. Conversely, in rigid fibrotic stroma, the cysteine cathepsins are down-regulated, leading to an accumulation of class IIa HDACs and suppression of MMP genes to favor tissue fibrosis. $n = 10$ human liver specimens (**A**). Original magnification, ×150. HAT, histone acetyltransferase; IKK, Iκ kinase; JNK, c-Jun N-terminal kinase; SMA, smooth muscle actin; TF, transcription factors.

Inverse Expression Pattern of HDAC4 and CtsH in the Fibrotic Septa of the Human Cirrhotic Liver

Finally, we examined the expression patterns of HDAC4 and CtsH in 10 human cirrhotic tissues, all derived from hepatitis C virus–mediated hepatocellular carcinoma. Immunofluorescence staining showed that, within the fibrotic septa, both HDAC4 and HDAC7 were highly expressed in the cells that also express α–smooth muscle actin, a marker of myofibroblastic HSCs (Figure 9A and Supplemental Figure S2). Conversely, CtsH was mostly absent within the fibrotic septa, but was detected in the nonfibrotic parenchyma (Figure 9A and Supplemental Figure S3). Such an inverse relationship between CtsH and HDAC4 levels was observed in most of the samples (8 of 10 human cirrhotic samples), and the results are consistent with the notions that CtsH negatively regulates HDAC4 and that suppression of CtsH is essential for maintaining high levels of HDAC4 in myofibroblastic HSCs in liver fibrosis (Figure 9B).

Discussion

We addressed two fundamental questions in the context of tissue injury, repair, and fibrosis. First, how do mesenchymal cells, including HSCs, sense the environmental ECM and respond to injury signals to turn on the expression of MMP genes in cases of acute injury? Second, how are the same MMP genes epigenetically silenced when the HSCs are transformed to myofibroblasts? Specifically, we addressed here how class IIa HDACs are down-regulated through a mechanism of proteolytic degradation in mesenchymal cells, including HSCs, residing in 3D ECM environment. We also addressed how down-regulation of class IIa HDACs may further configure the cells into an epigenetically permissive state, being ready for MMP expression when injury-signaling stimuli are present. Based on the evidence, we proposed a working mechanism to answer the two fundamental questions for the cell biology of tissue injury and fibrosis (Figure 9, B and C).

Initially, we speculated that the key signal-transduction pathways, including c-Jun N-terminal kinase and Iκ kinase, known for MMP gene activation, might be either up-regulated or down-regulated to accommodate the permissive and nonpermissive states in the normal liver and liver fibrosis, respectively. In contradiction to our initial expectation, the key signal-transduction pathways were neither additionally boosted by the cells at a permissive state (qHSCs) nor inactivated/suppressed in the myofibroblastic

HSCs.[8] Instead, the MMP genes were blocked and inaccessible, in line with impairment of histone acetylation and accumulation of HDAC4 in the myofibroblastic HSCs. Here, we extended the work, showing that the epigenetic machinery may be operated in two opposite modes for the permissive and nonpermissive states. In particular, our new evidence supports a theory that soft 3D ECM in the normal tissue context may confer the mesenchymal cells, including HSCs, into an epigenetically competent state, in part through up-regulating the cysteine-type cathepsins, which consequently break down the class IIa HDACs among others, leading to elevation of histone acetylation and setting an open configuration for many MMP genes, being ready for transcriptional activation on the IL-1/TNF-α–initiated injury-signaling pathways. Conversely, our work showed that, in fibrotic liver, the cysteine-type cathepsins are down-regulated in the activated HSCs, leading to accumulation of class II HDACs, which may consequently suppress the MMP genes, which ultimately promotes ECM accumulation in fibrogenesis.

The phenotypically permissive state, namely the epigenetic context in the healthy liver, by the HSCs within 3D ECM is additionally characterized showing cell cycle arrest at G_0 phase, cytoplasmic extensions, and storage of vitamin A droplets. An MMP locus containing 10 MMP genes, including two pseudo-genes, is located near the end arm of chromosome 8, whereas *MMP9* is located on chromosome 3. Most of these MMP genes are simultaneously up- and down-regulated in the permissive and the nonpermissive states, respectively. These synchronized actions indicate that a set of epigenetic mechanisms may operate in two opposite modes to accommodate the two opposite types of tissue environment: normal soft stroma and rigid fibrotic interface. However, DNA methylation in the promoters of two MMP genes (*MMP9* and *MMP13*) did not change in the time course of HSC *trans*-differentiation (L.Q.) when the MMP genes were fully silenced, thus precluding the role of DNA methylation in the early phase of MMP gene silencing in fibrogenesis. However, it is openly possible that DNA methylation and additional heterochromatin-like configuration may be applied for the later phase of suppression of the MMP loci.

The HDACs have emerged as key regulatory factors in tissue fibrosis.[19] Whereas most class I HDACs are ubiquitously expressed, the class IIa HDACs are versatile and have a more restricted pattern of expression in tissues and cells.[20] HDACs do not bind directly to DNA but are recruited to specific promoters through their interactions with DNA binding proteins, which are either cosuppressors, including CREB-binding protein/p300, or transcriptional factors, such as myocyte enhancer factor 2.[21,22] Subcellular localization of class II HDACs is also mediated by other signals, such as 14-3-3 proteins, calmodulin, heterochromatin protein 1, and SUMO.[23–25] In HSCs, but not in other mesenchymal cells, we often observed a high molecular band (about 230 kDa; Figure 1 and Supplemental Figure S1), which closely mirrors the full length of HDAC4. Through coimmunoprecipitation followed by Western blot analysis, we found that the 230-kDa band indeed was SUMO1-modified HDAC4. It would be of interest to investigate whether this modification is involved in the HDAC4-mediated functions in HSCs.

The turnover of class IIa HDACs can be affected by diverse physiologic conditions; the underlying mechanism appears to be cell type–dependent. For instance, caspase activation induced by UV irradiation or lipopolysaccharide treatment can alter HDAC4 turnover rate.[26–28] Classic ubiquitin/proteasome mechanisms are involved in HDAC4 degradation on serum starvation in certain cell types,[29,30] but not in the rat osteoblastic cell line.[31] To our knowledge, our study is the first to demonstrate cathepsin-dependent turnover of class IIa HDACs by mesenchymal cells in 3D ECM or HSCs in the quiescent state.

We have shown that HDAC4 degradation can be directly executed by cysteine-type cathepsins. Cysteine-type cathepsins are characterized primarily as lysosomal proteinases and require a reducing and acidic environment to execute proteolytic functions.[32] Indeed, we have shown that the CtsH/CtsL-mediated degradation of HDAC4 *in vitro* relies on acidic pH, and the results are in agreement with the *in vivo* data showing that chloroquine, which raises intracellular pH, blocks HDAC4 turnover. However, in addition to lysosomal location and nonspecific proteolysis, certain cathepsins were identified in other cellular compartments. For instance, a biochemically active CtsL variant that lacks N-terminal signal peptide has been found in the nuclei and cleaved CCAAT-displacement protein/Cut-related homeobox transcription factor and the N-terminus of histone H3 during mouse embryonic stem cell differentiation.[33,34] Nuclear localization of cysteine cathepsins may also be mediated through tethering with certain nuclear factors. In fact, our finding of physical binding of CtsH to HDAC4 supports this notion. Alternative translational initiation by the second ATG codon of the transcript may be another mechanism for the absence of cysteine cathepsins from the lysosomal destination. In this regard, CtsF has been detected in the nuclei of rat HSCs.[35] In addition, CtsK may be secreted and has been reported to be involved in ECM breakdown, and inactivation of CtsK has been identified in lung fibrosis.[36] CtsB has been reported to be involved in liver fibrosis.[37] In particular, Gressner et al[38] showed that the expression of cystatin C, an endogenous inhibitor of cathepsin, was increased during *trans*-differentiation of HSCs. The findings from those reports are consistent with our findings that cysteine cathepsins may localize to the nuclei, and that up-regulation of cysteine cathepsins in HSCs may be involved in down-regulation of other class IIa HDACs. Although our work has been mostly focused on CtsH, other cysteine cathepsins, in particular CtsL, may also mediate degradation of HDAC4 and other class II HDACs, and this notion should be further determined by experiment. As shown, CtsH-mediated degradation of HDAC4 may

occur in both cytoplasm and nuclei, and these results are consistent with the finding of punctate CtsH in the nuclei. Likewise, other class IIa HDACs, such as HDAC5 and HDAC7, may also serve as substrates for cysteine cathepsins. Additional work is needed to provide a complete understanding of cysteine cathepsins and substrate specificity involved in HSC *trans*-differentiation and functionality. Moreover, it is important to elucidate how environmental cues in the 3D ECM lead to up-regulation of cysteine cathepsins in the normal tissue stroma.

It is equally important to determine how the whole family of cysteine cathepsins is down-regulated at transcriptional levels by the cells on rigid interface. Cultivation of cells on plastic, as an extreme case to simulate the rigid mechanochemical force in fibrosis, is widely used for studying mesenchymal cell biology. The cells cultured on plastic dishes exhibit many key features that are also identified in cells of fibrotic tissues. For instance, the silencing of MMP genes observed in animal models of liver fibrosis was fully recapitulated by the HSCs activated on the plastic surface.[8] Moreover, in human cirrhotic liver samples, the suppression of cysteine cathepsins in the desmoplastic stroma was fully reconstituted by the activation of HSCs on plastic. Rigid and fibrotic interface activated cellular signals and promoted cell cycle transition to the S phase, but arrested in G_2/M phases (Z.Y., Y.L.). Others have shown that mechanosensitivity is crucial for signaling of transforming growth factor β, a prominent factor of tissue fibrosis.[39]

In conclusion, our work may explain the plasticity and responsiveness of mesenchymal cells in the ECM environment. As ECM degrading enzymes, the expression of MMP genes was examined here for their capacity to express in response to injury signals, and for their suppression in fibrosis. Many other genes and their functions should be regulated in a manner similar to that of the MMP genes in 3D ECM. Moreover, the epigenetic landscapes of the MMP loci by the mesenchymal cells should be mapped in detail for the permissive and nonpermissive states. Other epigenetic features, such as DNA and histone methylation, should also be reexamined for mesenchymal cells in 3D ECM. This information and knowledge may explain the functionality of mesenchymal cells in tissue environment.

Acknowledgment

We thank Professor Li Qintong (Sichuan University, Sichuan, China) for providing the F3777 and M2 antibodies.

Supplemental Data

Supplemental material for this article can be found at *http://dx.doi.org/10.1016/j.ajpath.2016.12.001*.

References

1. Friedman SL: Hepatic stellate cells: protean, multifunctional, and enigmatic cells of the liver. Physiol Rev 2008, 88:125−172
2. Yin C, Evason KJ, Asahina K, Stainier DY: Hepatic stellate cells in liver development, regeneration, and cancer. J Clin Invest 2013, 123: 1902−1910
3. Friedman SL: Liver fibrosis—from bench to bedside. J Hepatol 2003, 38(Suppl 1):S38−S53
4. Han YP, Zhou L, Wang J, Xiong S, Garner WL, French SW, Tsukamoto H: Essential role of matrix metalloproteinases in interleukin-1-induced myofibroblastic activation of hepatic stellate cell in collagen. J Biol Chem 2004, 279:4820−4828
5. Lu L, Feng M, Gu J, Xia Z, Zhang H, Zheng S, Duan Z, Hu R, Wang J, Shi W, Ji C, Shen Y, Chen G, Zheng SG, Han YP: Restoration of intrahepatic regulatory T cells through MMP-9/13-dependent activation of TGF-beta is critical for immune homeostasis following acute liver injury. J Mol Cell Biol 2013, 5:369−379
6. Seki E, De Minicis S, Osterreicher CH, Kluwe J, Osawa Y, Brenner DA, Schwabe RF: TLR4 enhances TGF-beta signaling and hepatic fibrosis. Nat Med 2007, 13:1324−1332
7. De Minicis S, Seki E, Uchinami H, Kluwe J, Zhang Y, Brenner DA, Schwabe RF: Gene expression profiles during hepatic stellate cell activation in culture and in vivo. Gastroenterology 2007, 132:1937−1946
8. Qin L, Han YP: Epigenetic repression of matrix metalloproteinases in myofibroblastic hepatic stellate cells through histone deacetylases 4: implication in tissue fibrosis. Am J Pathol 2010, 177:1915−1928
9. Choudhary C, Kumar C, Gnad F, Nielsen ML, Rehman M, Walther TC, Olsen JV, Mann M: Lysine acetylation targets protein complexes and co-regulates major cellular functions. Science 2009, 325:834−840
10. Verdin E, Dequiedt F, Kasler HG: Class II histone deacetylases: versatile regulators. Trends Genet 2003, 19:286−293
11. Niki T, Rombouts K, De Bleser P, De Smet K, Rogiers V, Schuppan D, Yoshida M, Gabbiani G, Geerts A: A histone deacetylase inhibitor, trichostatin A, suppresses myofibroblastic differentiation of rat hepatic stellate cells in primary culture. Hepatology 1999, 29:858−867
12. Glenisson W, Castronovo V, Waltregny D: Histone deacetylase 4 is required for TGFbeta1-induced myofibroblastic differentiation. Biochim Biophys Acta 2007, 1773:1572−1582
13. Mannaerts I, Eysackers N, Onyema OO, Van Beneden K, Valente S, Mai A, Odenthal M, van Grunsven LA: Class II HDAC inhibition hampers hepatic stellate cell activation by induction of microRNA-29. PLoS One 2013, 8:e55786
14. McKinsey TA, Zhang CL, Olson EN: Identification of a signal-responsive nuclear export sequence in class II histone deacetylases. Mol Cell Biol 2001, 21:6312−6321
15. Guncar G, Podobnik M, Pungercar J, Strukelj B, Turk V, Turk D: Crystal structure of porcine cathepsin H determined at 2.1 A resolution: location of the mini-chain C-terminal carboxyl group defines cathepsin H aminopeptidase function. Structure 1998, 6:51−61
16. Ueno T, Linder S, Na CL, Rice WR, Johansson J, Weaver TE: Processing of pulmonary surfactant protein B by napsin and cathepsin H. J Biol Chem 2004, 279:16178−16184
17. Han YP, Nien YD, Garner WL: Tumor necrosis factor-alpha-induced proteolytic activation of pro-matrix metalloproteinase-9 by human skin is controlled by down-regulating tissue inhibitor of metalloproteinase-1 and mediated by tissue-associated chymotrypsin-like proteinase. J Biol Chem 2002, 277:27319−27327
18. de Ruijter AJ, van Gennip AH, Caron HN, Kemp S, van Kuilenburg AB: Histone deacetylases (HDACs): characterization of the classical HDAC family. Biochem J 2003, 370:737−749
19. Pang M, Zhuang S: Histone deacetylase: a potential therapeutic target for fibrotic disorders. J Pharmacol Exp Ther 2010, 335:266−272
20. Yang XJ, Gregoire S: Class II histone deacetylases: from sequence to function, regulation, and clinical implication. Mol Cell Biol 2005, 25: 2873−2884

21. Bertos NR, Wang AH, Yang XJ: Class II histone deacetylases: structure, function, and regulation. Biochem Cell Biol 2001, 79:243–252
22. Han A, He J, Wu Y, Liu JO, Chen L: Mechanism of recruitment of class II histone deacetylases by myocyte enhancer factor-2. J Mol Biol 2005, 345:91–102
23. Grozinger CM, Schreiber SL: Regulation of histone deacetylase 4 and 5 and transcriptional activity by 14-3-3-dependent cellular localization. Proc Natl Acad Sci U S A 2000, 97:7835–7840
24. Wang AH, Kruhlak MJ, Wu J, Bertos NR, Vezmar M, Posner BI, Bazett-Jones DP, Yang XJ: Regulation of histone deacetylase 4 by binding of 14-3-3 proteins. Mol Cell Biol 2000, 20:6904–6912
25. McKinsey TA, Zhang CL, Olson EN: Activation of the myocyte enhancer factor-2 transcription factor by calcium/calmodulin-dependent protein kinase-stimulated binding of 14-3-3 to histone deacetylase 5. Proc Natl Acad Sci U S A 2000, 97:14400–14405
26. Liu F, Dowling M, Yang XJ, Kao GD: Caspase-mediated specific cleavage of human histone deacetylase 4. J Biol Chem 2004, 279: 34537–34546
27. Paroni G, Mizzau M, Henderson C, Del Sal G, Schneider C, Brancolini C: Caspase-dependent regulation of histone deacetylase 4 nuclear-cytoplasmic shuttling promotes apoptosis. Mol Biol Cell 2004, 15:2804–2818
28. Chen SW, Ma YY, Zhu J, Zuo S, Zhang JL, Chen ZY, Chen GW, Wang X, Pan YS, Liu YC, Wang PY: Protective effect of 1,25-dihydroxyvitamin D3 on ethanol-induced intestinal barrier injury both in vitro and in vivo. Toxicol Lett 2015, 237:79–88
29. Potthoff MJ, Wu H, Arnold MA, Shelton JM, Backs J, McAnally J, Richardson JA, Bassel-Duby R, Olson EN: Histone deacetylase degradation and MEF2 activation promote the formation of slow-twitch myofibers. J Clin Invest 2007, 117:2459–2467
30. Cernotta N, Clocchiatti A, Florean C, Brancolini C: Ubiquitin-dependent degradation of HDAC4, a new regulator of random cell motility. Mol Biol Cell 2011, 22:278–289
31. Shimizu E, Nakatani T, He Z, Partridge NC: Parathyroid hormone regulates histone deacetylase (HDAC) 4 through protein kinase A-mediated phosphorylation and dephosphorylation in osteoblastic cells. J Biol Chem 2014, 289:21340–21350
32. Eren F, Kurt R, Ermis F, Atug O, Imeryuz N, Yilmaz Y: Preliminary evidence of a reduced serum level of fibroblast growth factor 19 in patients with biopsy-proven nonalcoholic fatty liver disease. Clin Biochem 2012, 45:655–658
33. Goulet B, Baruch A, Moon NS, Poirier M, Sansregret LL, Erickson A, Bogyo M, Nepveu A: A cathepsin L isoform that is devoid of a signal peptide localizes to the nucleus in S phase and processes the CDP/Cux transcription factor. Mol Cell 2004, 14:207–219
34. Duncan EM, Muratore-Schroeder TL, Cook RG, Garcia BA, Shabanowitz J, Hunt DF, Allis CD: Cathepsin L proteolytically processes histone H3 during mouse embryonic stem cell differentiation. Cell 2008, 135:284–294
35. Maubach G, Lim MC, Zhuo L: Nuclear cathepsin F regulates activation markers in rat hepatic stellate cells. Mol Biol Cell 2008, 19: 4238–4248
36. Buhling F, Rocken C, Brasch F, Hartig R, Yasuda Y, Saftig P, Bromme D, Welte T: Pivotal role of cathepsin K in lung fibrosis. Am J Pathol 2004, 164:2203–2216
37. Canbay A, Guicciardi ME, Higuchi H, Feldstein A, Bronk SF, Rydzewski R, Taniai M, Gores GJ: Cathepsin B inactivation attenuates hepatic injury and fibrosis during cholestasis. J Clin Invest 2003, 112: 152–159
38. Gressner AM, Lahme B, Meurer SK, Gressner O, Weiskirchen R: Variable expression of cystatin C in cultured trans-differentiating rat hepatic stellate cells. World J Gastroenterol 2006, 12: 731–738
39. Cockerill M, Rigozzi MK, Terentjev EM: Mechanosensitivity of the 2nd kind: TGF-beta mechanism of cell sensing the substrate stiffness. PLoS One 2015, 10:e0139959

Supplemental Figure S1 Evidence showing potential small ubiquitin-like modifier (SUMO)-1 modification of histone deacetylase (HDAC)-4 by rat hepatic stellate cells (HSCs). Primary rat HSCs cultured on plastic for 6 days were subjected to immunoprecipitation (IP) with antibodies against HDAC4. Western blot (WB) analysis was applied to identify HDAC4 and its associated SUMO1. **Arrows** indicate full-length (140 kDa) HDAC4 and potential SUMO1-modified (approximately 230 kDa) HDAC4.

Supplemental Figure S2 Up-regulation of class IIa histone deacetylases (HDACs) in the fibrotic septa of human cirrhotic liver. Cirrhotic liver tissues from hepatocellular carcinoma patients were subjected to immunofluorescence staining analysis. **A:** Expression of class II HDACs, including HDAC4 and HDAC7, in the fibrotic septa is highlighted by coexpression of α—smooth muscle actin (SMA) in the human cirrhotic liver tissue. **B:** In one case, desmin, an intermediate filament marker for hepatic stellate cells (HSCs), was used for detecting the expression of HDAC4 in HSCs. $n = 10$ hepatocellular carcinoma patients (**A** and **B**). PT, patient.

Supplemental Figure S3 Down-regulation of cathepsin (CTS)-H in the fibrotic septa of human cirrhotic liver. Cirrhotic liver tissues from hepatocellular carcinoma patients were subjected to immunofluorescence staining analysis. Absence of CtsH expression in the fibrotic septa is indicated by the presence of α—smooth muscle actin (SMA) in the human cirrhotic liver tissue. Conversely, CtsH is expressed in the cells of the parenchyma outside of the fibrotic septa. $n = 10$ hepatocellular carcinoma patients. PT, patient.